GEOLOGY | THE GEOLOGICAL SOCIETY OF AMERICA®

https://doi.org/10.1130/G47282.1

Manuscript received 27 September 2019
Revised manuscript received 1 June 2020
Manuscript accepted 5 June 2020

Published online 21 July 2020

A test of the efficacy of sand saltation for silt production: Implications for the interpretation of loess

Steven M. Adams and Gerilyn S. Soreghan
School of Geosciences, University of Oklahoma, 100 E. Boyd Street, Norman, Oklahoma 73019, USA

ABSTRACT

Production of the silt that forms loess is attributed to processes operating in both glacial systems (glacial grinding) and sandy deserts (saltation-induced fracturing). However, the efficacy of saltation for significant silt production is controversial. Understanding the potential for silt production in deserts is essential for determining the paleoclimatic significance of loess. To better assess the significance of eolian abrasion for silt production, experimental abrasion was conducted in a device designed to simulate sand saltation at sustained storm-wind velocities (~25 m/s). The design differs from previous work in (1) maintaining strong measured velocities for long duration, (2) removing preexisting silt and utilizing control samples, (3) and scaling results to estimate potential for loess accumulation. Scaling experimental rates of production to geologic proportions indicates that eolian abrasion of sand produces insufficient silt to create geologically significant loess deposits.

INTRODUCTION

Silt composing many of Earth's major loess deposits is linked to physical grinding from glacial processes (e.g., Pye, 1995; Smalley, 1995; Assallay et al., 1998; Muhs, 2013). The desert loess hypothesis posits that the silt that forms loess originates largely by eolian abrasion of sand (e.g., Smalley and Vita-Finzi, 1968; Tsoar and Pye, 1987; Smith et al., 2002; Crouvi et al., 2008; Enzel et al., 2010), although Muhs (2013) noted that so-called "desert loess" could derive from deflation of silty sources (e.g., playas) or silt-rich protoliths.

Some assert that eolian abrasion plays a large role in silt production (Smith et al., 2002; Crouvi et al., 2008; Enzel et al., 2010). Evaluating the potential for silt generation by eolian abrasion (defined as intergranular collision during saltation) is fundamental to the use of loess as a paleoclimate indicator. If desert processes produce abundant silt, then loess in the geological record may have originated wholly or in part in deserts. If deserts do not produce significant silt in the loess size range through eolian abrasion, then desert-adjacent loess deposits likely contain silt produced by glaciation or other mechanisms.

Previous experiments have studied silt production by processes thought to operate in deserts, e.g., salt weathering and saltation abrasion (Kuenen, 1960; Goudie et al., 1979; Pye and Sperling, 1983; Smith and McGreevy, 1987; Whalley et al., 1987; Smith et al., 1991; Wright et al., 1998; Wright, 2001; Bullard et al., 2004, 2007; Marshall et al., 2012; Swet et al., 2019). Experiments designed to test the efficacy of silt production by intergranular collisions have yielded varying results, from negligible (Kuenen, 1960; Swet et al., 2019) to substantial silt (Whalley et al., 1987; Smith et al., 1991; Wright et al., 1998; Wright, 2001; Bullard et al., 2004, 2007; Bullard and White, 2005), with the latter cited as supporting evidence for the hypothesis that sandy deserts produce silt to form loess (Smith et al., 2002; Crouvi et al., 2008; Enzel et al., 2010).

Here, we focused on silt (operationally defined as 5–63 µm) experimentally created from saltation-induced fracturing of eolian sand under simulated natural wind speeds. These experiments maintained strong storm winds (~25 m/s) over relatively long intervals (up to 8 d), enabling representative scaling of geologically significant parameters. Results address the potential for saltation-induced fracturing to produce sufficient silt to form loess, and thus bear on the enduring controversy of "desert versus glacial" origins for geologically significant loess.

METHODS

Sand samples of ~2 kg each were collected from dune crests at the upwind margins of the Algodones (California, USA) and Little Sahara (Oklahoma) dune fields for abrasion experiments (Tables S1 and S2 in the Supplemental Material[1]). Samples were wet sieved to remove grains <250 µm. The <63 µm fraction was measured with a Malvern Mastersizer 3000 laser particle-size analyzer (LPSA). The >250 µm fraction was split, with one half designated as "unwashed," and the other designated as "washed." Washed samples were agitated in 5% $(NaPO_3)_6$ dispersant to remove clay and oxide coatings. For each of the four starting sample types, four 100 g aliquots were subjected to experimental abrasion, and one 100 g sample was designated as a control. The experimental aliquots were abraded for 1, 2, 4, and 8 d. Three additional Little Sahara washed 4 d samples were abraded for reproducibility, with processing to reduce loss (fewer transfers between containers) during sample collection and measurement. Grain size was measured for unprocessed bulk samples using LPSA (Table S2). The starting material was subsampled for grain size and mineralogical analyses (Tables S2 and S3). The >250 µm fraction used in abrasion was measured by LPSA. Point counts ($n = 400$) on the four types of starting material revealed the mineralogy.

[1]Supplemental Material. Table S1 (GPS coordinates of sample locations), Table S2 (grain-size distribution data; https://doi.pangaea.de/10.1594/pangaea.914301), Table S3 (point-counting data), Table S4 (automated surface observing stations [ASOS] GPS and wind data), Table S5 (scaling methods and detailed calculation), Table S6 (law of wall calculation and plot), and Table S7 (control sample mass loss). Please visit https://doi.org/10.1130/GEOL.S.12555545 to access the supplemental material, and contact editing@geosociety.org with any questions.

CITATION: Adams, S.M., and Soreghan, G.S., 2020, A test of the efficacy of sand saltation for silt production: Implications for the interpretation of loess: Geology, v. 48, p. 1105–1109, https://doi.org/10.1130/G47282.1

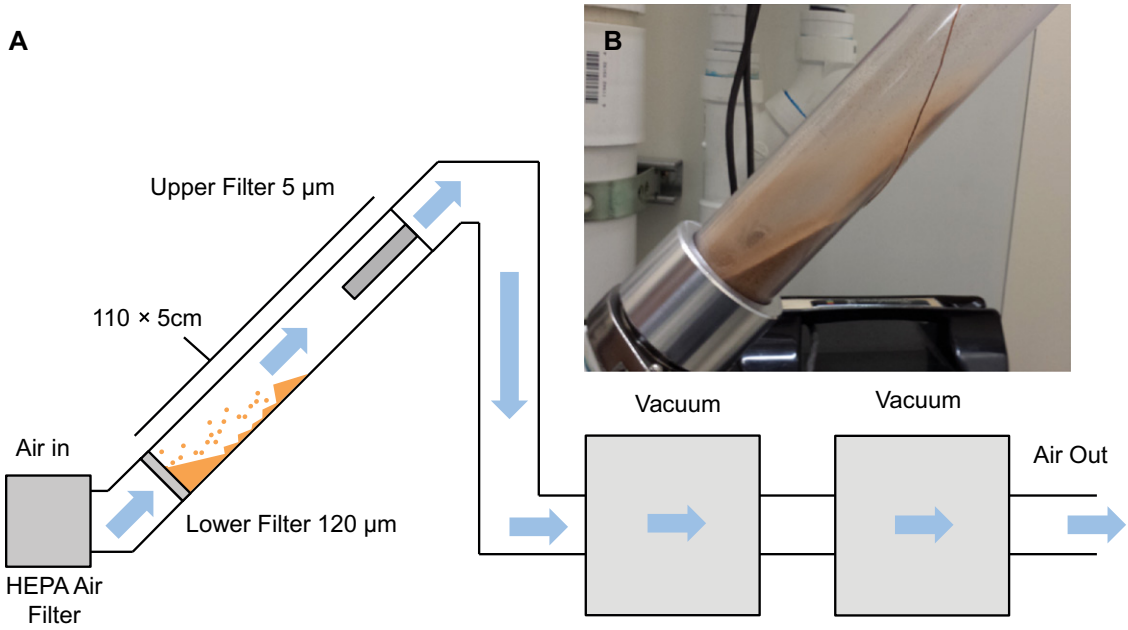

Figure 1. Eolian abrasion device. (A) Schematic diagram of device with air-flow directions (blue arrows). Air is pulled through the chamber at ~25 m/s. Sand blown upward in the chamber descends and collides with upward-blowing sand. (B) Photograph of device chamber during operation. Arc of blown sand is colliding with returning sand pulses. HEPA—high-efficiency particulate air.

Abrasion Device

The experimental device (Fig. 1) employed two vacuum motors to create an air flow of 3–35 m/s in an inclined (60°), 5-cm-diameter polycarbonate chamber equipped with steel-mesh filters at the base (120 µm) and top (5 µm). While grains <5 µm technically could pass through the upper filter, they do not; rather, they cling to the filter owing to electrostatic formation of aggregates >5 µm. Sand placed in the chamber prior to operation settled into a pseudo-dune, wedge shape at the chamber base (Fig. 1). An antistatic spray prevented particles from clinging to chamber walls.

Chamber air velocity was measured using a hotwire anemometer with and without sand present to determine velocity ranges and associated hop distance of sand under experimental conditions. This hop distance was marked on the chamber, and the motors were adjusted to maintain this distance, and the corresponding velocity. If the hop distance of the sand diminished, the power was increased. A peak wind speed of 25 m/s was selected as representative of severe dust storms (Zhou and Wang, 2002), and thus the most extreme natural conditions. Wind velocities varied slightly from 20 to 25 m/s (measured 2 cm above surface) during experiments owing to sand migration.

At the end of each run, dust was collected from both filters, and the emptied chamber was rinsed with distilled water to collect all particles. All materials were sieved to separate sand (>63 µm), silt (operationally, grains passing the 63 µm sieve and retained on the 5 µm sieve), and clay (operationally, grains that passed the 5 µm sieve) particles. Silt and clay fractions were weighed prior to LPSA analysis. Table 1 lists masses and size modes of produced silt.

Method for Scaling Results

The scaling method converted experimental results to a potential maximum of silt produced by a dune field annually. Maximum annual duration for storm-wind speeds in a desert was determined using weather station data from windy regions (Oklahoma, Texas, and Wyoming [USA], and China; NOAA National Climatic Data Center, 2018; Table S4). The windiest location averaged 322 h above

TABLE 1. MASS AND GRAIN-SIZE RESULTS

Sample	Number of days	Silt 5–63 µm mass* (g)	Grain-size vol% mode (µm)	Clay mass (g)	Sand mass (g)	Loss mass (g)
Algodones washed						
AL-WS-C	0	0.0000	BDL§	0	99.7778	0.2222
AL-WS-1D	1	0.0018	41.9	0	99.8301	0.1681
AL-WS-2D	2	0.0019	58.9	0.0034	99.5541	0.4406
AL-WS-4D2	4	0.0014	45.6	0.0184	99.6086	0.3716
AL-WS-8D	8	0.0037	35.3	0.0296	99.5941	0.3726
Algodones unwashed						
AL-OR-C	0	0.0000	BDL	0	99.7050	0.2950
AL-OR-1D	1	0.0002	BDL	0.0032	99.4031	0.5935
AL-OR-2D	2	0.0003	BDL	0.0063	99.7735	0.2199
AL-OR-4D2	4	0.0010	31.1	0.0437	99.5493	0.4060
AL-OR-8D	8	0.0011	40.1	0.0476	99.4854	0.4659
Little Sahara washed						
LS-WS-C	0	0.0000	BDL	0	99.9437	0.0563
LS-WS-1D	1	0.0001	BDL	0.0009	99.8534	0.1456
LS-WS-2D	2	0.0001	BDL	0.0024	99.8079	0.1896
LS-WS-4D1	4	0.0026	51.8	0.0105	99.7641	0.2228
LS-WS-4D2	4	0.0058	43.1	0	99.6951	0.2991
LS-WS-4D3	4	0.0039	36.7	0	99.7557	0.2404
LS-WS-4D4	4	0.0046	50.1	0	99.7756	0.2198
LS-WS-8D	8	0.0036	45.6	0.0175	99.8391	0.1398
Little Sahara unwashed						
LS-RD-C	0	0.0004	BDL	0	99.8312	0.1684
LS-RD-1D	1	0.0000	BDL	0.002	99.6918	0.3062
LS-RD-2D	2	0.0009	35.3	0.0119	99.6999	0.2873
LS-RD-4D	4	0.0011	27.4	0.0083	99.8051	0.1855
LS-RD-8D	8	0.0025	35.3	0.0636	99.4700	0.4639
Algodones field sites						
AL-S8	NA†	NA	79.0	NA	NA	NA
AL-S3	NA	NA	83.6	NA	NA	NA
AL-S7	NA	NA	75.5	NA	NA	NA
Little Sahara field sites						
LS-S1	NA	NA	73.5	NA	NA	NA
LS-S4	NA	NA	77.8	NA	NA	NA
LS-S5	NA	NA	77.2	NA	NA	NA

Note: WS—washed samples; BDL—below detectable level; RD and OR—unwashed samples. Control sample and bulk sediment grain-size modes: AL-WS-C (368 µm); AL-OR-C (393 µm); LS-WS-C (426 µm); LS-RD-C (425 µm); AL-S8 (336 µm); LS-1 (297 µm). Average lost mass of control samples and additional error tests: 0.2347 g (see Table S7 [see text footnote 1]).

*Starting mass was 100 g, so silt mass produced in grams equates to the % starting mass.

†NA—not applicable.

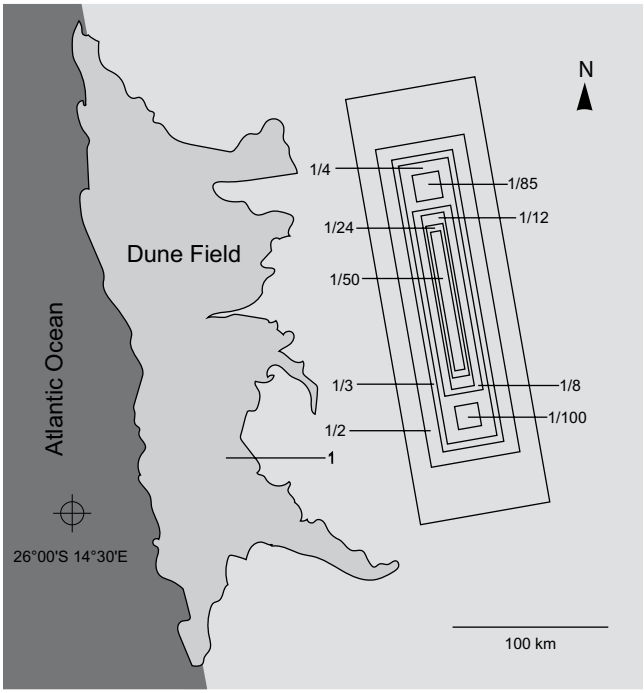

Figure 2. Namib Desert and surface areas of potential loess. Loess deposit surface areas are fractions of the parent dune field surface area (rectangles). Table 2 lists accumulation rates for each loess deposit. At 1/85th of the area of parent desert, the loess deposit meets the accumulation rate proposed by Pye (1984) needed to exceed erosion and soil formation.

20 m/s (measured at 10 m) annually, so we chose 400 h as an upper limit of annual wind speed durations above 20 m/s. Choosing a higher annual average provides a conservative estimate for (1) remote desert locations that are windy but have no Automated Surface Observing Stations (ASOS) stations, and (2) potentially gustier Pleistocene deserts (McGee et al., 2010).

A 100 g mass of sand with a density of 1.65 g/cm^3 can be represented as a 2.4 cm × 2.5 cm × 10 cm block (60 cm^3). This volume and surface area equate to that of the sand wedge in the experimental chamber. Assuming a dune field always maintains a sand depth >2.4 cm, the surface area and annual abrasion duration at storm velocities are the key dimensions for scaling. These yield the amount of silt produced annually by 25 cm^2 of surface area under maximized conditions. To scale these results, we used the surface area of a dune field. The Namib dune system was chosen to illustrate the scaling method because (1) it is a large, continuous dune field expected to produce abraded fines, (2) it has readily defined borders enabling area measurement, and (3) it has small loess deposits downwind (Brunotte and Heinz, 2000). Given the area, the maximum amount of silt can be calculated by

$$\frac{m_e}{A_e} = \frac{m_d}{A_d}, \quad (1)$$

where m_e is mass of experimental silt, m_d is mass of desert silt, A_e is surface area of experimental sand in the chamber, and A_d is surface area of sand in the desert. The experimental mass was calculated using the silt mass produced by sample LS-WS-4D2 (the sample with the highest mass produced) and assuming a linear production rate of 400 h of device abrasion. Depositional rates can be calculated for theoretical loess using the produced silt mass results. Several rates were calculated for deposits using a fractional area of the parent dune field as measured in Google Earth™ (Fig. 2; Table 2; Table S5).

RESULTS AND DISCUSSION

Table 1 lists grain-size modes and masses of size classes. Table 2 presents the vertical and mass accumulation rates (VARs and MARs) for theoretical deposits with surface areas that are fractions of the parent desert surface area. Table S2 lists grain-size distributions of silt and sand.

TABLE 2. RATES TO ACCUMULATE 1 M OF LOESS OVER A FRACTION OF THE AREA OF PARENT DESERT (NAMIB 32,385 km^2)

	Fraction of parent area								
Rate	1/2 area	1/3 area	1/4 area	1/8 area	1/12 area	1/24 area	1/50 area	1/85 area	1/100 area
VAR (mm/yr)	0.01	0.018	0.023	0.05	0.07	0.14	0.29	0.50	0.59
MAR (g/m^2/yr)	19.33	29.00	38.67	77.33	116.00	232.00	483.33	821.67	966.67
Time required (yr)	85,344	56,897	42,672	21,336	14,224	7112	3414	2008	1707

Note: VAR—vertical accumulation rate over given area; MAR—mass accumulation rate over given area. Time required is number of years needed to accumulate 1 m of loess over given area. Proposed required VAR for loess formation from Pye (1984) is 0.5 mm/yr.

Silt Mass and Grain Size

The mass of silt produced was significantly lower, in terms of both total mass and percentage of starting material, compared to most previous studies (Whalley et al., 1987; Smith et al., 1991; Wright et al., 1998; Wright, 2001; Bullard et al., 2004, 2007). Likely explanations for the difference include (1) use of natural sand and removal of preexisting fines, (2) chamber design, which minimized collisions with chamber walls to focus on saltation-induced intergranular collisions, (3) use of realistic and monitored wind speeds, and (4) use of softer polycarbonate rather than glass for the experimental chamber, thus eliminating artificial production of fines.

Two studies that produced more silt used crushed Brazilian vein quartz for the starting material, which has an angularity prone to chipping and spalling of protuberances (Whalley et al., 1987; Wright et al., 1998). In contrast, natural dune sand realistically mimics a dune system. Additionally, with the exception of one or two samples in Bullard et al. (2004) and Swet et al. (2019), respectively, all previous studies using natural dune sand used samples containing preexisting fines. We removed preexisting fines from all samples, and control samples were also processed to measure potential fines that survived sieving. We posit that the substantial silt produced in previous experiments using natural dune sand (Bullard et al., 2004, 2007) reflects the ready release of preexisting fines in the experimental device. Hence, we think the calculations by Amit et al. (2014) that relied on the silt production rates of Whalley et al. (1987) and Bullard et al. (2004) likely overestimated the capacity of deserts to produce silt by saltation fracturing.

With the exception of Swet et al. (2019), no previous studies have controlled for, nor measured, wind speed within the abrasion chambers; rather, they introduced compressed air, likely producing an overly energetic and thus unrealistically abrasive environment relative to natural dune systems. The ~20–25 m/s velocity we used aligns with the most energetic sustained winds experienced in average dust storms in deserts, excluding short gusts (Liu et al., 2005), and significantly exceeds velocities (8.5 m/s) used by Swet et al. (2019). Given that energy scales positively with velocity squared (Krinsley and Wellendorf, 1980; Marshal et al., 2012), and saltation flux scales with velocity cubed (Bagnold, 1941), the high velocities (20–25 m/s) induced a much higher potential for silt creation, as more sand grains were saltating in more energetic collisions. This implies that the potential for silt creation via saltation is much lower at typical wind speeds experienced in dune fields.

The weather stations used in this study measure wind velocity at a height of 10 m. Given the logarithmic decline in velocity approaching the surface (law of the wall), the values recorded at or above 20 m/s would produce lower velocities

near ground level, where grains collide with the bed. Scaling up from 2 cm height (measured in the chamber) to 10 m, 20 m/s in the chamber corresponds to ~40 m/s recorded by a weather station (Table S6). Marshall et al. (2012) placed the required velocity for large-scale chipping and spalling at ~17–19 m/s, depending on grain shape, whereas Krinsley and Wellendorf (1980) estimated 40 m/s. Both of these previous experiments used crushed Brazilian quartz and inferred that saltation at most natural wind speeds would not produce silt by saltation breakage. This imparts confidence that our experiments provide a conservative estimate of the energy experienced by most saltating grains, even in extreme climates, including the Pleistocene, which might have had a higher frequency of gusty events (McGee et al., 2010).

Our experimentally produced silt exhibit grain-size distributions consistent with other studies (Wright et al., 1998; Bullard et al., 2004, 2007). The modal range of the produced silt (23–52 μm) falls in the range of the Peoria loess (Wang et al., 2006) and (coarser modes of) West African offshore dust (8–42 μm; Stuut et al., 2005), but it is coarser than typical Chinese loess (~25 μm) and finer than silt at North African desert margins (~60 μm; Assallay et al., 1998). The modes of the experimentally produced silt were finer than the modes of the preexisting particles removed from our starting material (66.9–76.0 μm for Algodones, 73.5–77.8 μm for Little Sahara).

Our samples consisted of quartz as well as potentially abrasion-prone phases such as feldspars and lithics (Table S3), consistent with typical dune sands of the Namib (Garzanti et al., 2012). Yet, results showed minimal evidence for abrasion despite the presence of these relatively fragile phases. This raises the issue of potential limitations to our approach, which include the (necessarily) limited number of sample locations and abrasion tests, and any effects of removing the fine fraction. However, the samples are typical eolian quartzose sand with similar durability to average dune sand. Previous experiments are similarly limited in terms of sample numbers.

Scaling

Table 2 lists the accumulation rates (ARs) for fractional areas of the Namib dune field. These values assume no loss from erosion after deposition, and they assume that all silt that is produced accumulates, which is a conservative overestimate. The ARs extrapolated from the experimental results maximize silt production since they: (1) assume abrasion with equal vigor everywhere, whereas—realistically—energy varies spatially across a desert, and distal rounding and fining of sand produce a downwind reduction in abrasion potential as protuberances are removed, and (2) employ the highest rate of silt produced in the experiments.

After scaling to maximize silt produced, the results indicate that depositional rates are extremely low until the area of deposition is <1/85th the area of the parent desert (Table 2). Using 0.5 mm/yr as the minimum VAR required to produce a recognizable loess deposit (Pye, 1984), the results imply that a desert loess deposit requires a parent dune field ~85 times larger than the area of loess accumulation. While the minimum rate would vary locally depending on rates of erosion and pedogenesis, our results imply that silt production by eolian abrasion is insufficient to outpace soil formation and erosion, and thus these processes are unlikely to form geologically significant loess deposits. For very large dune fields, where produced silt could be effectively concentrated and accumulated, small adjacent loess deposits are possible; e.g., the northern Nigerian loess is thought to originate by deflation of fines from the Chad Basin (McTainsh, 1987).

CONCLUSIONS

Experimental eolian saltation of natural sands using realistic wind speeds and conservative scaling of production rates indicates that eolian sand saltation is unlikely to produce geologically significant loess. Although silt in loess could contain a small fraction of material produced from eolian abrasion of sand, the majority of silt in loess likely originated via other processes. These results suggest that formation of loess composed of silt generated by eolian sand saltation requires—at minimum—an active dune field with a surface area nearly two orders of magnitude larger than the loess deposit. For extensive loess deposits in the geological record, the absence of evidence for such a parent dune field, or the need for a dune field of unreasonably large dimensions should raise the possibility that the silt originated via different processes. Viable processes include glacial grinding, deflation of silt-rich exposed delta systems, and/or derivation from silt-rich precursors. The difficulty of making voluminous loess from sand saltation suggests that geographically extensive primary loess deposits (e.g., comparable to the Chinese Loess Plateau) might be unlikely or unable to form in the absence of glaciation.

ACKNOWLEDGMENTS

Funding was provided by the National Science Foundation (EAR-1338331 and OISE 1658614), the Eberly Family Chair, University of Oklahoma, the Society for Sedimentary Geology (SEPM; student grant), and the Geological Society of America (student grant). We thank J. Young for aid in design/construction of the device; Leeman Geophysical, LLC, for acquisition of wind speed data; and Joe Mason, M. Sweeney, and several anonymous reviewers for constructive comments.

REFERENCES CITED

Amit, R., Enzel, Y., Mushkin, A., Gillespie, A., Batbaatar, J., Crouvi, O., Vandenberghe, J., and An, Z., 2014, Linking coarse silt production in Asian sand deserts and Quaternary accretion of the Chinese Loess Plateau: Geology, v. 42, p. 23–26, https://doi.org/10.1130/G34857.1.

Assallay, A.M., Rogers, C.D.F., Smalley, I.J., and Jefferson, I.F., 1998, Silt: 2–62 μm, 9–4φ: Earth Science Reviews, v. 45, p. 61–88, https://doi.org/10.1016/S0012-8252(98)00035-X.

Bagnold, R.A., 1941, The Physics of Blown Sand and Desert Dunes: London, Methuen & Co. Ltd., 265 p.

Brunotte, E., and Sander, H., 2000, Loess accumulation and soil formation in Kaokoland (northern Namibia) as indicators of Quaternary climatic change: Global and Planetary Change, v. 26, p. 67–75, https://doi.org/10.1016/S0921-8181(00)00034-5.

Bullard, J.E., and White, K., 2005, Dust production and the release of iron oxides resulting from the aeolian abrasion of natural dune sands: Earth Surface Processes and Landforms, v. 30, p. 95–106, https://doi.org/10.1002/esp.1148.

Bullard, J.E., McTainsh, G.H., and Pudmenzky, C., 2004, Aeolian abrasion and modes of fine particle production from natural red dune sands: An experimental study: Sedimentology, v. 51, p. 1103–1125, https://doi.org/10.1111/j.1365-3091.2004.00662.x.

Bullard, J.E., Mctainsh, G.H., and Pudmenzky, C., 2007, Factors affecting the nature and rate of dust production from natural dune sands: Sedimentology, v. 54, p. 169–182, https://doi.org/10.1111/j.1365-3091.2006.00827.x.

Crouvi, O., Amit, R., Enzel, Y., Porat, N., and Sandler, A., 2008, Sand dunes as a major proximal dust source for late Pleistocene loess in the Negev Desert, Israel: Quaternary Research, v. 70, p. 275–282, https://doi.org/10.1016/j.yqres.2008.04.011.

Enzel, Y., Amit, R., Crouvi, O., and Porat, N., 2010, Abrasion-derived sediments under intensified winds at the latest Pleistocene leading edge of the advancing Sinai-Negev erg: Quaternary Research, v. 74, p. 121–131, https://doi.org/10.1016/j.yqres.2010.04.002.

Garzanti, E., Andò, S., Vezzoli, G., Lustrino, M., Boni, M., and Vermeesch, P., 2012, Petrology of the Namib Sand Sea: Long-distance transport and compositional variability in the wind-displaced Orange Delta: Earth-Science Reviews, v. 112, p. 173–189, https://doi.org/10.1016/j.earscirev.2012.02.008.

Goudie, A.S., Cooke, R.U., and Doornkamp, J.C., 1979, The formation of silt from quartz dune sand by salt-weathering processes in deserts: Journal of Arid Environments, v. 2, p. 105–112, https://doi.org/10.1016/s0140-1963(18)31786-5.

Krinsley, D., and Wellendorf, W., 1980, Wind velocities determined from the surface textures of sand grains: Nature, v. 283, p. 372–373, https://doi.org/10.1038/283372a0.

Kuenen, P.H., 1960, Experimental abrasion 4 : Eolian action: The Journal of Geology, v. 68, p. 427–449, https://www.jstor.org/stable/30084814.

Marshall, J.R., Bull, P.A., and Morgan, R.M., 2012, Energy regimes for aeolian sand grain surface textures: Sedimentary Geology, v. 253–254, p. 17–24, https://doi.org/10.1016/j.sedgeo.2012.01.001.

McGee, D., Broecker, W.S., and Winckler, G., 2010, Gustiness: The driver of glacial dustiness?: Quaternary Science Reviews, v. 29, p. 2340–2350, https://doi.org/10.1016/j.quascirev.2010.06.009.

McTainsh, G., 1987, Desert loess in northern Nigeria: Zeitschrift für Geomorphologic, v. 31, p. 145–165.

Muhs, D.R., 2013, The geologic records of dust in the Quaternary: Aeolian Research, v. 9, p. 3–48, https://doi.org/10.1016/j.aeolia.2012.08.001.

National Oceanic and Atmospheric Administration (NOAA) National Climatic Data Center, 2018, Automated Surface Observing System (ASOS): 1-Minute ASOS Data: NOAA National Centers for Environmental Information, https://www.ncdc.noaa.gov/data-access/land-based-station-data/land-based-datasets/automated-surface-observing-system-asos (accessed 29 April 2018).

Pye, K., 1984, Some perspectives on loess accumulation: Loess Letters, v. 11, p. 5–10.

Pye, K., 1995, The nature, origin and accumulation of loess: Quaternary Science Reviews, v. 14, p. 653–667, https://doi.org/10.1016/0277-3791(95)00047-X.

Pye, K., and Sperling, C.H.B., 1983, Experimental investigation of silt formation by static breakage processes: The effect of temperature, moisture and salt on quartz dune sand and granitic regolith: Sedimentology, v. 30, p. 49–62, https://doi.org/10.1111/j.1365-3091.1983.tb00649.x.

Smalley, I., 1995, Making the material: The formation of silt sized primary mineral particles for loess deposits: Quaternary Science Reviews, v. 14, p. 645–651, https://doi.org/10.1016/0277-3791(95)00046-1.

Smalley, I.J., and Vita-Finzi, C., 1968, The formation of fine particles in sandy deserts and the nature of "desert" loess: Journal of Sedimentary Petrology, v. 38, p. 766–774, https://doi.org/10.1306/74D71A69-2B21-11D7-8648000102C1865D.

Smith, B.J., McGreevy J.P., and Whalley, W.B., 1987, Silt production by weathering of a sandstone under hot arid conditions: An experimental study: Journal of Arid Environments, v. 12, p. 199–214, https://doi.org/10.1016/S0140-1963(18)31164-9.

Smith, B.J., Wright, J.S., and Whalley, W.B., 1991, Simulated aeolian abrasion of Pannonian sands and its implications for the origins of Hungarian loess: Earth Surface Processes and Landforms, v. 16, p. 745–752, https://doi.org/10.1002/esp.3290160808.

Smith, B.J., Wright, J.S., and Whalley, W.B., 2002, Sources of non-glacial, loess-size quartz silt and the origins of "desert loess": Earth-Science Reviews, v. 59, p. 1–26, https://doi.org/10.1016/S0012-8252(02)00066-1.

Stuut, J.B., Zabel, M., Ratmeyer, V., Helmke, P., Schefuß, E., Lavik, G., and Schneider, R., 2005, Provenance of present-day eolian dust collected off NW Africa: Journal of Geophysical Research: Atmospheres, v. 110, D04202, https://doi.org/10.1029/2004JD005161.

Swet, N., Elperin, T., Kok, J.F., Martin, R.L., Yizhaq, H., and Katra, I., 2019, Can active sands generate dust particles by wind-induced processes?: Earth and Planetary Science Letters, v. 506, p. 371–380, https://doi.org/10.1016/j.epsl.2018.11.013.

Tsoar, H., and Pye, K., 1987, Dust transport and the question of desert loess formation: Sedimentology, v. 34, p. 139–153, https://doi.org/10.1111/j.1365-3091.1987.tb00566.x.

Wang, H., Mason, J.A., and Balsam, W.L., 2006, The importance of both geological and pedological processes in control of grain size and sedimentation rates in Peoria Loess: Geoderma, v. 136, p. 388–400, https://doi.org/10.1016/j.geoderma.2006.04.005.

Whalley, W.B., Smith, B.J., McAlister, J.J., and Edwards, A.J., 1987, Aeolian abrasion of quartz particles and the production of silt-size fragments: Preliminary results, *in* Frostick, L.E., and Reid, I., eds., Desert Sediments: Ancient and Modern: Geological Society [London] Special Publication 35, p. 129–138, https://doi.org/10.1144/GSL.SP.1987.035.01.09.

Wright, J., 2001, Making loess-sized quartz silt: Data from laboratory simulations and implications for sediment transport pathways and the formation of "desert" loess deposits associated with the Sahara: Quaternary International, v. 76–77, p. 7–19, https://doi.org/10.1016/S1040-6182(00)00085-9.

Wright, J., Smith, B., and Whalley, B., 1998, Mechanisms of loess-sized quartz silt production and their relative effectiveness: Laboratory simulations: Geomorphology, v. 23, p. 15–34, https://doi.org/10.1016/S0169-555X(97)00084-6.

Zhou, Z., and Wang, X., 2002, Analysis of the severe group dust storms in eastern part of Northwest China: Journal of Geographical Sciences, v. 12, p. 357–362, https://doi.org/10.1007/BF02837557, https://link.springer.com/content/pdf/10.1007/BF02837557.pdf (accessed April 2018).

Printed in USA